Journal of Nuclear Materials 377 (2008) 409–414

Contents lists available at ScienceDirect

Journal of Nuclear Materials

journal homepage: www.elsevier.com/locate/jnucmat

Low-temperature thermally-activated deformation and irradiation softening in neutron-irradiated molybdenum

Meimei Li *, T.S. Byun, L.L. Snead, S.J. Zinkle

Materials Science and Technology Division, Oak Ridge National Laboratory, Oak Ridge, TN 37831, United States

ARTICLE INFO

Article history:
Received 14 December 2007
Accepted 28 March 2008

ABSTRACT

The effect of neutron irradiation on low-temperature deformation of Mo in two heat treatments, i.e. annealed and stress-relieved, was investigated. Specimens were irradiated at reactor coolant temperature (~80 °C) to doses ranging from 7.2×10^{-5} to 0.28 dpa in the High Flux Isotope Reactor. Tensile tests were carried out between −50 and 100 °C at strain rates of 1×10^{-5}–1×10^{-2} s^{-1}. Thermal activation analysis based on tensile data was performed to understand the low-temperature deformation mechanism. Irradiation softening and reduced dependence on test temperature and strain rate of the yield stress was observed in the annealed Mo after low-dose neutron irradiation (<~0.003 dpa). Higher dose neutron irradiation caused athermal hardening only. The stress-relieved Mo showed a weaker dependence on test temperature and strain rate of the yield stress than the annealed Mo, and the dependence of the yield stress of the stress-relieved Mo was nearly unchanged after irradiation. Comparison of the experimental values of activation parameters with the theoretical predictions of dislocation models indicates that the Fleischer model of interactions of dislocations with tetragonal strains gave a better description of the activation process than the double-kink model, which implies a scavenging effect. The reduced test temperature and strain rate dependence following irradiation may be explained by the decreased effective stress due to trapping of interstitial solute species by neutron-produced defects.

1. Introduction

It has been widely accepted that neutron irradiation at low temperature will lead to an increase in the yield strength of a metal or alloy, i.e. 'irradiation hardening'. More and more experimental evidence has shown that low-temperature neutron irradiation can also lead to a decrease in yield strength, i.e. 'irradiation softening'. Irradiation softening has been observed in several bcc metals, including Fe, Mo, V, at low test temperatures and/or high strain rates [1–7]. For example, Mo experienced irradiation softening when tested below room-temperature after neutron irradiation to low-doses (10^{-3} dpa) at 80 °C [7]. This irradiation-induced softening has led to reduced stress-temperature dependence in neutron-irradiated Mo compared to unirradiated Mo. As irradiation softening occurred only at low test temperatures and/or high strain rates, a routine room-temperature test at a typical strain rate such as 10^{-3} s^{-1} often does not capture this effect.

The finding of 'irradiation softening' was closely related to the test temperature and strain rate dependence of flow stresses and the associated thermally-activated deformation mechanisms in irradiated bcc metals and alloys. The strong dependence of flow stresses on test temperature and strain rate distinguishes bcc from fcc and hcp materials, and it is linked directly to the ductile-brittle transition temperature (DBTT). It is known that the yield stress of a bcc metal increases significantly with decreasing test temperatures or increasing strain rates at low temperatures, typically below 0.1–0.2 T_m (T_m is the melting point of the metal or alloy) [8]. The transition between brittle and ductile fracture occurs when the strongly temperature-dependent yield stress is greater than the less temperature-sensitive fracture stress [9]. As the fracture stress is insensitive to neutron irradiation at low doses [10–12], the effect of neutron irradiation on the temperature dependence of the yield stress is the key factor that influences the shift of the DBTT under irradiation. Irradiation softening and its accompanied reduced temperature dependence of the yield stress may improve low-temperature ductility.

Irradiation softening is often discussed with reference to bcc 'alloy softening' that has similar nature [13,14]. 'Alloy softening' has been observed in bcc alloys where small additions of alloying elements decrease the temperature dependence of the flow stresses, and at low test temperatures, the yield stress of the alloy is even lower than that of the base metal [14]. This phenomenon is also called 'solid solution softening'. The 'alloy softening' effect has been well studied in bcc transition metals, particularly in the refractory VIA group metals Cr, Mo and W [15–19]. It may be used as a possible way to improve low-temperature ductility of refractory metals, such as the so-called 'rhenium ductilizing effect'

* Corresponding author. Present address: Nuclear Engineering Division, Argonne National Laboratory, 9700 South Cass Avenue, Argonne, IL 60439-4838, United States. Tel.: +1 630 2525111; fax: +1 630 2523604.
E-mail address: mli@anl.gov (M. Li).

0022-3115/$ - see front matter © 2008 Elsevier B.V. All rights reserved.
doi:10.1016/j.jnucmat.2008.03.017

[19]. The 'alloy softening' effect has been explained by extrinsic theories such as the scavenging model where the alloy addition removes interstitial atoms from solution, leading to a reduction in yield stress; the effect was also suggested to originate from intrinsic factors, e.g. the lattice resistance to dislocation motion, or the Peierls stress, and the double-kink mechanism is the rate-controlling deformation mechanism [14,20–22]. The theories of 'alloy softening' have been applied to 'irradiation softening', as both phenomena are associated with thermally-activated dislocation glide mechanisms [13,23]. There is a significant debate whether intrinsic or extrinsic factors dominate.

Irradiation softening and decreased test temperature dependence of the yield stress in neutron-irradiated Mo was described by the Fleischer model of interactions of dislocations with tetragonal strain fields in our previous work [7]. A similar softening effect was observed in neutron-irradiated Mo by Tanaka et al. [6], and the effect was suggested to be attributed to the strain fields associated with irradiation-induced defect clusters that assist the formation of double kinks in the screw dislocation. To better understand this low-temperature thermally-activated deformation process in Mo, the present work determined the activation parameters from tensile data obtained over different test temperatures and at a wide range of strain rates. The results were compared with predictions of various dislocation models. This paper also presents the tensile data for irradiated Mo in the stress-relieved condition, and compares them with tensile results previously reported for annealed Mo [7,24,25].

2. Experimental procedure

The material examined was low-carbon arc-cast (LCAC) Mo with purity >99.95% and interstitial impurity contents of 140 wppm C, 6 wppm O and 8 wppm N. Two specimen geometries were used, subsize SS-3 sheet tensile specimens with gauge dimensions of $7.62 \times 1.52 \times 0.50$ mm and subsize SS-1 sheet tensile specimens with gauge dimensions of $20.32 \times 1.27 \times 0.50$ mm. Prior to neutron irradiation, the SS-3 tensile specimens were annealed at 1200 °C/1 h to obtained equiaxed grain structure with a grain size of ~70 μm; the SS-1 tensile specimens were stress-relieved (900 °C/1 h), resulting in elongated grains with a grain size of ~2 μm in the transverse direction.

Irradiation was carried out at reactor coolant temperature (~80 °C) in the hydraulic tube facility of the High Flux Isotope Reactor (HFIR) at the Oak Ridge National Laboratory. Specimens in the annealed condition were irradiated to seven neutron fluences in the range of 2×10^{21} to 8×10^{24} n/m^2 ($E > 0.1$ MeV), corresponding to displacement damage levels of 7.2×10^{-5}, 7.2×10^{-4}, 0.003, 0.0072, 0.03, 0.072 and 0.28 dpa. Specimens in the stress-relieved condition were irradiated to neutron fluences of 8×10^{22} n/m^2 and 8×10^{23} n/m^2 ($E > 0.1$ MeV), corresponding to displacement damage doses of 0.003 and 0.03 dpa.

Tensile tests were conducted at temperatures ranging from −50 to 100 °C at strain rates between 1×10^{-5} and 1×10^{-2} s^{-1} in air or a mixed air and cold nitrogen environment. Unirradiated annealed Mo was also tested at −100 °C and at a strain rate of 1×10^{-1} s^{-1}.The details of tensile test conditions are given in Table 1. Load and displacement data were recorded and used to determine stress–strain curves and tensile properties.

Microstructural characterization of as-irradiated specimens and as-irradiated and deformed specimens and SEM fractography were reported in the references [24,25].

3. Results

3.1. Effect of heat treatment on test temperature and strain rate dependence of the yield stress and the plastic instability stress

The temperature dependence of the yield stress and the true stress at the ultimate tensile strength, so-called plastic instability stress (PIS), is shown in Fig. 1(a) for unirradiated Mo in the annealed and stress-relieved conditions. The strain rate dependence at room temperature is given in Fig. 1(b). Literature data on annealed and stress-relieved Mo [6,26,27] are included in Fig. 1 for comparison. The yield stress of annealed Mo showed strong test temperature and strain rate dependence. The yield stress increased significantly when the test temperature was decreased and the strain rate was increased. The threshold temperature, T_0 or an athermal temperature, above which the stress becomes nearly temperature-independent, is about 200 °C (0.16 T_m). The PIS of annealed Mo was less sensitive to test temperature and strain rate than the yield stress.

The heat treatment significantly affected the dependence of the yield stress on the test temperature and strain rate. The stress-relieved Mo showed weaker test temperature and strain rate dependence of the yield stress than the annealed material. In fact, the

Table 1
Tensile test conditions

Heat treatment	Dose (dpa)	Test temperature (°C)	Strain rate (1/s)	Heat treatment	Dose (dpa)	Test temperature (°C)	Strain rate (1/s)
Annealed	0	−100	1×10^{-3}	Annealed	0.0072	22	1×10^{-3}
Annealed	0	−50	1×10^{-3}	Annealed	0.0072	100	1×10^{-3}
Annealed	0	−25	1×10^{-3}	Annealed	0.03	22	1×10^{-3}
Annealed	0	100	1×10^{-3}	Annealed	0.03	22	1×10^{-4}
Annealed	0	22	1×10^{-3}	Annealed	0.03	22	1×10^{-5}
Annealed	0	22	1×10^{-1}	Annealed	0.072	−50	1×10^{-3}
Annealed	0	22	1×10^{-2}	Annealed	0.072	−25	1×10^{-3}
Annealed	0	22	1×10^{-4}	Annealed	0.072	22	1×10^{-3}
Annealed	0	22	1×10^{-5}	Annealed	0.072	100	1×10^{-3}
Annealed	7.2×10^{-5}	−50	1×10^{-3}	Annealed	0.28	22	1×10^{-3}
Annealed	7.2×10^{-5}	−25	1×10^{-3}	Annealed	0.28	100	1×10^{-3}
Annealed	7.2×10^{-5}	22	1×10^{-3}	Stress-relieved	0	22	1×10^{-2}
Annealed	7.2×10^{-5}	100	1×10^{-3}	Stress-relieved	0	22	1×10^{-3}
Annealed	7.2×10^{-4}	−50	1×10^{-3}	Stress-relieved	0	22	1×10^{-4}
Annealed	7.2×10^{-4}	22	1×10^{-3}	Stress-relieved	0	22	1×10^{-5}
Annealed	7.2×10^{-4}	100	1×10^{-3}	Stress-relieved	0.003	22	1×10^{-2}
Annealed	0.003	22	1×10^{-2}	Stress-relieved	0.003	22	1×10^{-3}
Annealed	0.003	22	1×10^{-3}	Stress-relieved	0.003	22	1×10^{-4}
Annealed	0.003	22	1×10^{-4}	Stress-relieved	0.003	22	1×10^{-5}
Annealed	0.003	22	1×10^{-5}	Stress-relieved	0.03	22	1×10^{-3}
Annealed	0.0072	−50	1×10^{-3}	Stress-relieved	0.03	22	1×10^{-4}
Annealed	0.0072	−25	1×10^{-3}	Stress-relieved	0.03	22	1×10^{-5}

test temperature and strain rate dependence of the yield stress of the stress-relieved Mo was close to that of the PIS for the annealed Mo.

The yield stress and the PIS of Mo follow a single semi-logarithmic relationship to the strain rate, as shown in Fig. 1(b), i.e.,

$$\sigma = k_1 + k_2 \log(\mathrm{d}\varepsilon/\mathrm{d}t) \quad (1)$$

where σ is the yield stress or the PIS, $(\mathrm{d}\varepsilon/\mathrm{d}t)$ is the strain rate, and k_1 and k_2 are the constants. The strain rate sensitivity (SRS) of stresses at room temperature is given by the constant, k_2:

$$\left(\frac{\Delta\sigma}{\Delta \ln(\mathrm{d}\varepsilon/\mathrm{d}t)}\right)_T = \frac{k_2}{2.3} \quad (2)$$

The SRS of the yield stress was high in the annealed material, and it was decreased by either heat treatment (e.g. the stress-relieved Mo showed a smaller SRS) or by plastic deformation (e.g. the SRS of the PIS was smaller than the SRS of the yield stress in the annealed Mo).

3.2. Effect of neutron irradiation on test temperature and strain rate dependence of the yield stress and the PIS

Fig. 2 shows the test temperature dependence of the yield stress and the PIS of annealed Mo neutron-irradiated at 80 °C to doses between 7.2×10^{-5} and 0.28 dpa [25]. All the tensile tests were performed at a strain rate of $1 \times 10^{-3}\ \mathrm{s}^{-1}$. Neutron irradiation at lower doses decreased the yield stress of Mo when tested below room temperature, and slightly increased the yield stress at the test temperature of 100 °C, leading to a reduced temperature dependence of the yield stress. The maximum irradiation-induced softening occurred at ~0.001 dpa. Neutron irradiation to higher doses significantly increased the yield stress without further reduction of its temperature dependence. In contrast to the yield stress, the PIS was not affected by neutron irradiation in either magnitude or dependence on the test temperature. There was a trend for the temperature dependence of the yield stress to be reduced to the same level as of the PIS by low-dose neutron irradiation, and further irradiation caused only athermal hardening.

The strain rate dependence of the yield stress and the PIS of Mo neutron-irradiated at 80 °C to 0.003 and 0.03 dpa are shown in Fig. 3 for two heat treatments, annealed and stress-relieved. Similar to the temperature dependence, the strain rate dependence of the yield stress of the annealed material decreased after irradiation due to irradiation softening at higher strain rates and irradiation hardening at lower strain rates. The yield stress of the annealed Mo decreased after irradiation to 0.003 dpa when the specimens were tested at a strain rate above $1 \times 10^{-2}\ \mathrm{s}^{-1}$. Irradiation to 0.03 dpa significantly increased the yield stress and caused severe embrittlement, resulting in a decrease in the yield stress with strain rate. Again, neutron irradiation did not affect the PIS when tested at various strain rates. The stress-relieved specimens did not show irradiation softening, and the temperature dependence of the yield stress was nearly unchanged by neutron irradiation, indicating athermal hardening in the stress-relieved condition. Comparing the tensile data for the annealed and stress-relieved Mo irradiated to 0.03 dpa, it is evident that the stress-relieved Mo showed better resistance to irradiation embrittlement than the annealed Mo.

The dose dependence of irradiation softening and irradiation hardening is shown in Fig. 4 for annealed and stress-relieved Mo tested at room temperature. It is evident that softening occurred after irradiation to doses <~0.003 dpa and hardening occurred at higher doses. It should be noted that the irradiation softening effect depends on irradiation dose, test temperature and strain rate.

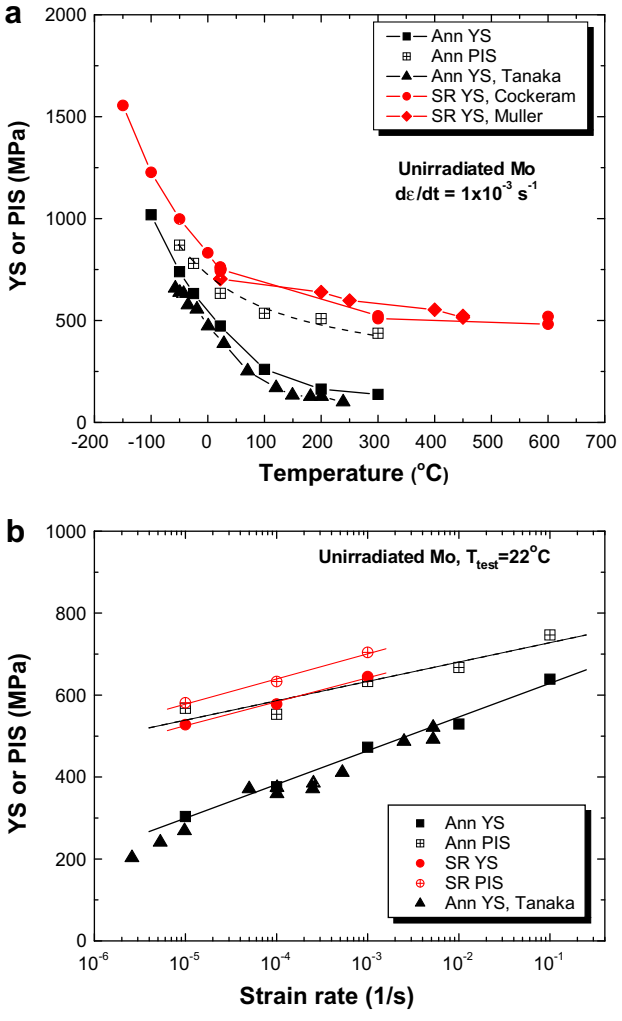

Fig. 1. Effect of heat treatment on (a) test temperature dependence of the yield stress (YS) and the plastic instability stress (PIS) of unirradiated Mo and (b) strain rate dependence of the YS and the PIS of unirradiated Mo.

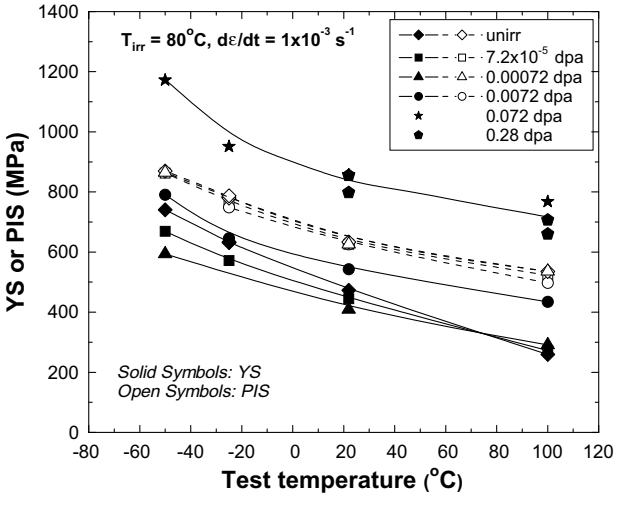

Fig. 2. Test temperature dependence of the yield stress (YS) and the plastic instability stress (PIS) of annealed Mo in unirradiated and irradiated conditions (strain rate of $1 \times 10^{-3}\ \mathrm{s}^{-1}$).

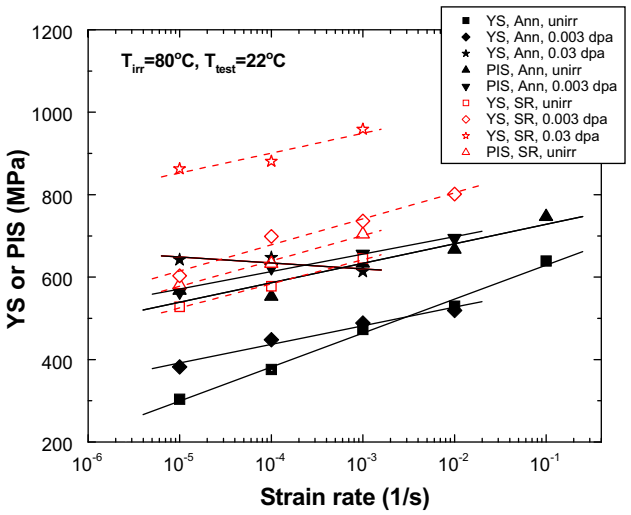

Fig. 3. Strain-rate dependence of the yield stress (YS) and the plastic instability stress (PIS) of unirradiated and irradiated Mo.

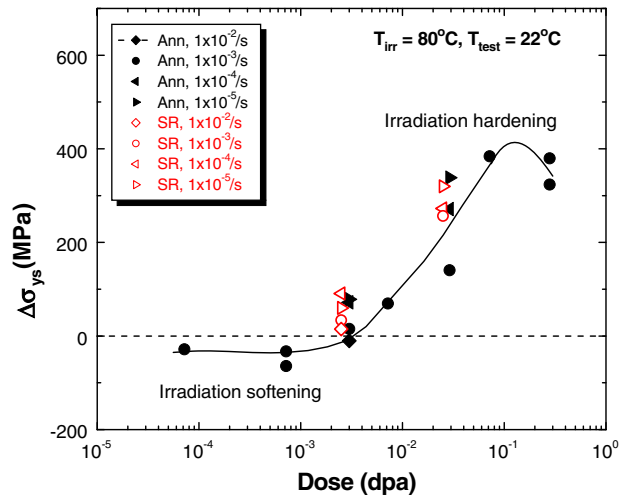

Fig. 4. Dose dependence of irradiation softening and irradiation hardening in Mo at a test temperature of 22 °C for two heat treatment conditions.

4. Thermal activation analysis

A thermally-activated deformation mechanism may be understood through 'thermal activation analysis' [8,28–31]. For a single thermally-activated deformation process, the rate equation is given by

$$(\mathrm{d}\varepsilon/\mathrm{d}t) = (\mathrm{d}\varepsilon_0/\mathrm{d}t)\exp\left(-\frac{G(\sigma^*)}{kT}\right) \tag{3}$$

where $(\mathrm{d}\varepsilon_0/\mathrm{d}t)$ is a parameter that depends on the mobile dislocation density, vibrational frequency, strain per successful activation, and entropy, $G(\sigma^*)$ is the activation energy as a function of the effective stress, σ^*, k is the Boltzmann's constant and T is the absolute temperature. The effective stress, σ^* refers to the thermal component of the applied stress, which is associated with short-range barriers and gives strong temperature dependence. It is defined as

$$\sigma^* = \sigma - \sigma_\mu \tag{4}$$

where σ is the applied stress (note that $\sigma = M\tau$, M is Taylor's factor and τ is the resolved shear stress), and σ_μ is the athermal stress associated with long-range barriers, and its temperature dependence is the same as for the shear modulus. The activation volume, V^* is defined as the negative stress derivative of the activation energy [8,28–31]

$$V^* = -M\cdot\left(\frac{\partial G}{\partial\sigma^*}\right)_T = M\cdot kT\left(\frac{\partial\ln(\mathrm{d}\varepsilon/\mathrm{d}t)}{\partial\sigma^*}\right)_T \tag{5}$$

The activation volume measures the work done by the external stress during the activation process, and it can be determined experimentally. Another important parameter that can be obtained from experiments is the activation enthalpy, H that represents the energy provided by thermal fluctuation to overcome short-range barriers during the rate-controlling process. A thermodynamic analysis of the rate equation gives that [8,28–31]

$$H = -kT^2\left(\frac{\partial\sigma^*}{\partial T}\right)_{(\mathrm{d}\varepsilon/\mathrm{d}t)}\left(\frac{\partial\ln(\mathrm{d}\varepsilon/\mathrm{d}t)}{\partial\sigma^*}\right)_T \tag{6}$$

According to Eqs. (5) and (6), experimental data of the strain-rate and temperature dependence of the yield and flow stresses will give the activation volume and the activation enthalpy.

The activation volume, V^* of Mo was determined using Eq. (5) and the strain rate sensitivity of the flow stress obtained from the room-temperature tensile data. Fig. 5 shows the activation volume as a function of true plastic strain and applied stress, respectively, for the unirradiated and irradiated Mo in annealed and stress-relieved conditions. The activation volume either increased

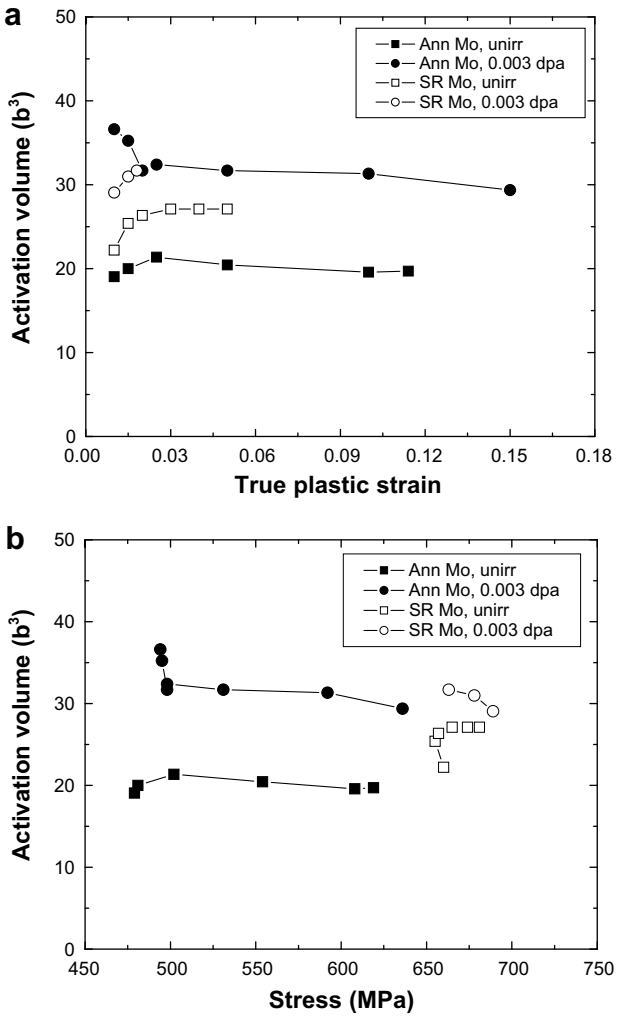

Fig. 5. Activation volume as a function of (a) true plastic strain and (b) stress in unirradiated and irradiated Mo in two heat treatments.

Table 2
Estimation of the activation enthalpy from experimental data

Specimen condition	Heat treatment	Effective stress (MPa)	Activation enthalpy (eV)
Unirradiated	Annealed	335[a]	0.74
0.003 dpa	Annealed	234[a]	0.88
Unirradiated	Stress-relieved	252[a]	0.83
0.003 dpa	Stress-relieved	202[a]	0.97
Unirradiated	Annealed	194[b]	1.05
0.003 dpa	Stress-relieved	217[b]	0.94

[a] The yield stress.
[b] The PIS.

or decreased with increasing plastic strain near the yield point and reached a stable value at a plastic strain of ~0.02 with the values varying between 20 and 30 b^3 (b is the Burgers vector, 0.273 nm for Mo), as shown in Fig. 5(a). When the activation volume was plotted as a function of applied stress in Fig. 5(b), it is clearly seen that V^* was increased by heat treatment or by neutron irradiation to a similar level.

The activation enthalpy, H, of the yield stress and the PIS at room temperature for the unirradiated and the 0.003 dpa specimens was determined from the experimental data using Eq. (6), and the values are given in Table 2. An approximation was made that the differential partial $(\partial\sigma^*/\partial T)$ of the 0.003 dpa specimens was the same as the 0.0072 dpa specimens, justified by the fact that only athermal hardening occurred above 0.003 dpa, as shown in Fig. 2. The effective stress, σ^*, shown in Table 2 was separated from the measured stress, σ by estimating the athermal stress as explained in our earlier paper [7]. Compared to the annealed-unirradiated Mo, which showed the largest test temperature and strain rate dependence, the effective stress was decreased and the activation enthalpy was increased in other conditions. The activation enthalpy, H at room temperature was between 0.74 and 1.05 eV.

5. Discussion

The dependence of the yield stress of the annealed Mo on test temperature and strain rate was decreased by low-dose neutron irradiation. Related to the reduced test temperature and strain rate dependence was irradiation softening observed at lower test temperatures and at higher strain rates. The dependence of the yield stress in the stress-relieved Mo was already low in the unirradiated condition relative to the annealed Mo, the dependence was nearly unchanged by neutron irradiation, and only irradiation hardening was observed. Due to limited irradiation and test conditions for the stress-relieved Mo, we can not rule out irradiation softening that may occur at a very low dose and/or at a very low test temperature. It is expected that any irradiation softening in the stress-relieved Mo would be smaller than in the annealed Mo. It was also found that the PIS of Mo was insensitive to neutron irradiation, and the dependence of the PIS on test temperature and strain rate appears to be characteristic reflecting the lowest dependence of the yield and flow stresses in Mo.

At a given stress, the activation volume of Mo was increased to nearly the same level, either by neutron irradiation, e.g. the annealed −0.003 dpa specimens, or by heat treatments, e.g. the stress-relieved specimens with or without neutron irradiation (see Fig. 5). This implies that a similar rate-controlling deformation process was operating in the irradiated and the stress-relieved Mo. We had shown previously that the temperature dependence of the yield stress in the unirradiated and irradiated Mo may be modeled by Fleischer's theory [7]. In the Fleischer model, temperature-dependent hardening was explained through the interactions of dislocations and tetragonal strain fields associated with interstitials, divacancies, point defect-impurity complexes and small dislocation loops, and the activation enthalpy as a function of the effective stress is given as [32,33]

$$H = H_0\left[1 - \left(\frac{\sigma^*}{\sigma_0^*}\right)^{0.5}\right]^2 \tag{7}$$

where H_0 is the activation enthalpy at $\sigma^* = 0$, and σ_0^* is the effective stress at 0 K. When the experimental values of the activation enthalpy given in Table 2 are plotted as a function of the effective shear stress and fitted by Eq. (7) as shown in Fig. 6, good agreement between the predicted values and the experimental values is obtained with $H_0 = 1.66$ eV (~0.1 μb^3), and $\sigma_0^* = 3600$ MPa. The value of σ_0^* is close to the extrapolated value for the 0.00072 dpa specimen [7]. The activation enthalpy, 1.66 eV (~0.1 μb^3), indicates solution effects in Mo [34].

Another model predicting activation parameters is the double-kink model, in which the Peierls stress is overcome by formation of a pair of kinks assisted by thermal fluctuation, and once a critical energy is exceeded, the kinks separate and carry the dislocation segment forward by one atomic spacing. Seeger [35] developed a model to determine the activation enthalpy for this deformation process

$$H = H_K\left[1 + 0.25\log\left(\frac{16\sigma_p^0}{\pi\sigma^*}\right)\right] \tag{8}$$

where H_K is the energy of a single kink at zero stress, and σ_p^0 is the Peierls stress at 0 K. From the literature [31,36], the value of H_K is about 0.6 eV for pure Mo. The Peierls stress for bcc metals, σ_p^0 is given as [21]

$$\sigma_p^0 = M\cdot\alpha\frac{\mu}{2}\exp\left(-\frac{2\pi\gamma}{b}\right) \tag{9}$$

where α is a constant related to the periodic force varying from 0.5 to 1, γ is the dislocation 'width' equal to half the lattice constant, and μ is the shear modulus. The kink-pair formation enthalpy may also be determined by Seeger's elastic-interaction model that is valid for small effective stresses [37]

$$H = 2H_K - \sqrt{2a^3b\gamma_0\sigma^*} \tag{10}$$

where a is the kink height (~0.43 nm for pure Mo [36]), γ_0 is an elastic contribution factor (7.88×10^{-10} N for pure Mo [36]). The calculated values of the activation enthalpy for Mo from Eqs. (8)–(10) are shown in Fig. 6, and compared with experimental data.

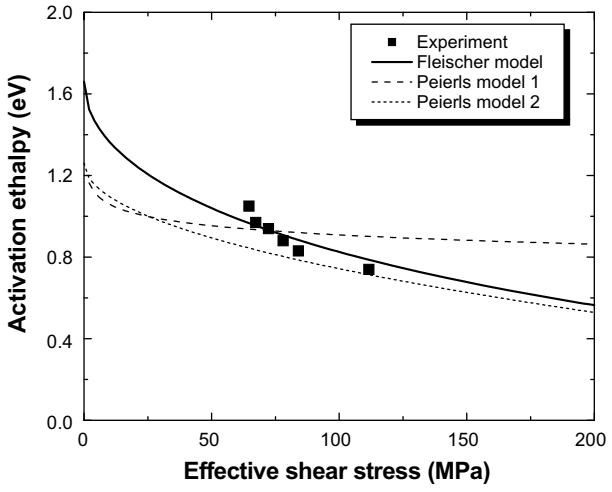

Fig. 6. Comparison of activation enthalpy obtained from experimental data and calculated by the Fleischer model and the Peierls model (Peierls model 1 is Eq. (8) and Peierls model 2 is Eq. (10)).

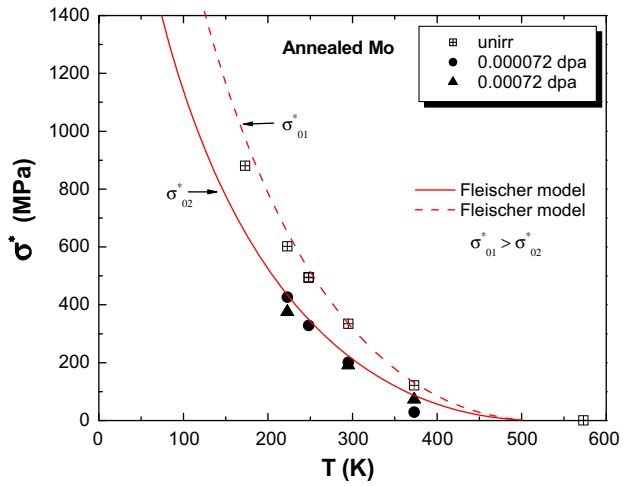

Fig. 7. Comparison of theoretical curve of the Fleischer model with experimental data of the effective stress as a function of test temperature. Irradiation softening and the reduced test temperature and strain rate dependence at low doses may be explained by the decreased effective stress.

The activation analysis indicates that the Fleischer model gave a better description of the activation process of the low-temperature deformation in irradiated Mo than the double-kink model.

The temperature dependence of the effective stress can be calculated using the following equation of the Fleischer model [23]:

$$\sigma^* = \sigma_0^* \left[1 - \sqrt{\frac{kT}{H_0} \ln \frac{A}{(\mathrm{d}\varepsilon/\mathrm{d}t)}} \right]^2 \tag{11}$$

Fig. 7 compares the experimental data of the effective stress with the theoretical values obtained from Eq. (11) with the same activation enthalpy and the critical stress used in Fig. 6. A good fit was found between the experiment and the prediction. Irradiation softening and the reduced test temperature and strain rate dependence after neutron irradiation may be explained by the decreased effective stress, as indicated in Fig. 7, and impurity interstitials act as short-range barriers to thermally-activated dislocation motion. The impurity interstitials in solution may be removed by neutron irradiation-induced defects, resulting in a smaller effective stress. The trapping of interstitial impurities by dislocations may also occur in the stress-relieved specimens where the number density of dislocations was much higher than in the annealed specimens. The same explanation can account for the smaller temperature dependence of the PIS than the yield stress.

6. Conclusions

Irradiation softening and reduced test temperature and strain rate dependence of the yield stress was observed in annealed Mo after low-dose neutron irradiation (<~0.003 dpa). The dependence of the yield stress on test temperature and strain rate was decreased to the same level as of the PIS prior to absolute athermal hardening, while the PIS was insensitive to neutron irradiation. Stress-relieved Mo exhibited a smaller dependence of the yield stress on the test temperature and the strain rate than annealed Mo. Neutron irradiation had little or no influence on test temperature and strain rate dependence of stress-relieved Mo. Thermal activation analysis of the deformation process indicated that the Fleischer model of interactions of dislocations with tetragonal strain fields describes the activation process better than the double-kink model, which implies a scavenging mechanism. Irradiation softening and reduced test temperature and strain rate dependence in Mo may be explained by the decreased effective stress due to trapping of interstitial solute species by irradiation-produced defects.

Acknowledgements

The research was sponsored by the Office of Fusion Energy Sciences, the US Department of Energy under Contract DE-AC05-00OR22725 with Oak Ridge National Laboratory, managed and operated by UT-Battelle, LLC. The authors would like to thank Drs. F.W. Wiffen and R.L. Klueh for their technical reviews. The authors would also like to express their appreciation to J.L. Bailey, A.M. Williams, L.T. Gibson and P.S. Tedder for their technical support.

References

[1] E. Pink, R.J. Arsenault, Radiat. Eff. 10 (1971) 27.
[2] H. Matsui, H. Shimidzu, S. Takehana, M.W. Guinan, J. Nucl. Mater. 155–157 (1988) 1169.
[3] K. Kitajima, H. Abe, Y. Aono, E. Kuramoto, S. Takamura, J. Nucl. Mater. 108&109 (1982) 436.
[4] P. Groh, F. Vanoni, P. Moser, Defects and Defect Clusters in B.C.C. Metals and Their Alloys, August 1973, p. 19.
[5] S. Takamura, Radiat. Eff. Lett. 57 (1980) 115.
[6] M. Tanaka, K. Fukaya, K. Shiraishi, Trans. JIM 20 (1979) 697.
[7] Meimei Li, T.S. Byun, N. Hashimoto, L.L. Snead, S.J. Zinkle, J. Nucl. Mater. 371 (2007) 53.
[8] G. Taylor, Prog. Mater. Sci. 36 (1992) 29.
[9] G.E. Dieter, Mechanical Metallurgy, second Ed., McGraw-Hill Book Company., 1976.
[10] M.S. Wechsler, in: The Interaction of Radiation with Solids, North-Holland, Amsterdam, 1964, p. 246.
[11] E.V. van Osch, M.I. de Vries, J. Nucl. Mater. 271&272 (1999) 162.
[12] E.V. van Osch, M.G. Horsten, M.I. de Vries, J. Nucl. Mater. 258–263 (1998) 301.
[13] M.S. Wechsler, in: R. De Batist, J. Nihoul, L. Stals, (Ed.), Defects in Refractory Metals, 1972, p. 257.
[14] E. Pink, R.J. Arsenault, Prog. Mater. Sci. 24 (1979) 1.
[15] B.C. Allen, R.I. Jaffee, Trans. Am. Soc. Metals 56 (1963) 387.
[16] J.R. Stephens, W.R. Witzke, J. Less-Common Met. 23 (1971) 325.
[17] J.R. Stephens, W.R. Witzke, J. Less-Common Met. 29 (1972) 371.
[18] J.R. Stephens, W.R. Witzke, J. Less-Common Met. 41 (1975) 265.
[19] W. Klopp, J. Less-Common Met. 42 (1975) 261.
[20] H. Suzuki, in: F.R.N. Nabarro (Ed.), Dislocations in Solids, vol. 4, North-Holland, Amsterdam, 1979.
[21] R.J. Arsenault, Acta Metall. 15 (1967) 501.
[22] A. Sato, M. Meshii, Acta Metall. 21 (1973) 753.
[23] R.J. Arsenault, Acta Metall. 15 (1967) 1853.
[24] Meimei Li, N. Hashimoto, T.S. Byun, L.L. Snead, S.J. Zinkle, J. Nucl. Mater. 367–370 (2007) 817.
[25] M. Li, M. Eldrup, T.S. Byun, N. Hashimoto, L.L. Snead, S.J. Zinkle, J. Nucl. Mater. 376 (2008) 11.
[26] B.V. Cockeram, J.L. Hollenbeck, L.L. Snead, J. Nucl. Mater. 324 (2004) 77.
[27] G.V. Műller, PhD Thesis, Lausanne, EPFL, 1997.
[28] G. Schoeck, Phys. Stat. Sol. 8 (1965) 499.
[29] A.G. Evans, R.D. Rawlings, Phys. Stat. Sol. 34 (1969) 9.
[30] H. Conrad, H. Wiedersich, Acta Metall. 8 (1960) 128.
[31] H. Conrad, W. Hayes, Trans. ASM 56 (1963) 249.
[32] R.L. Fleischer, J. Appl. Phys. 33 (1962) 3504.
[33] R.L. Fleischer, Acta Metall. 10 (1962) 835.
[34] H.J. Frost, M.F. Ashby, Deformation-Mechanism Maps: The Plasticity and Creep of Metals and Ceramics, Pergamon (1982).
[35] A. Seeger, Phil. Mag. 1 (1956) 651.
[36] L. Hollang, M. Hommel, A. Seeger, Phys. Stat. Sol. (a) 160 (1997) 329.
[37] A. Seeger, in: P. Veyssiere, L. Kubin, J. Castaing (Eds.), Dislocations 1984, Editions C.N.R.S., Paris, 1984, p. 141.